RAPID REPORT

An *in vivo* tethered toxin approach for the cell-autonomous inactivation of voltage-gated sodium channel currents in nociceptors

Annika S. Stürzebecher[1], Jing Hu[2], Ewan St John Smith[2], Silke Frahm[1], Julio Santos-Torres[1], Branka Kampfrath[1], Sebastian Auer[1], Gary R. Lewin[2] and Inés Ibañez-Tallon[1]

[1]*Molecular Neurobiology group,* [2]*Molecular Physiology of Somatic Sensation, Department of Neuroscience, Max-Delbrück Center for Molecular Medicine, Robert-Rössle Strasse 10, 13125 Berlin, Germany*

The Journal of Physiology

Understanding information flow in sensory pathways requires cell-selective approaches to manipulate the activity of defined neurones. Primary afferent nociceptors, which detect painful stimuli, are enriched in specific voltage-gated sodium channel (VGSC) subtypes. Toxins derived from venomous animals can be used to dissect the contributions of particular ion currents to cell physiology. Here we have used a transgenic approach to target a membrane-tethered isoform of the conotoxin MrVIa (t-MrVIa) only to nociceptive neurones in mice. T-MrVIa transgenic mice show a $44 \pm 7\%$ reduction of tetrodotoxin-resistant (TTX-R) VGSC current densities. This inhibition is permanent, reversible and does not result in functional upregulation of TTX-sensitive (TTX-S) VGSCs, voltage-gated calcium channels (VGCCs) or transient receptor potential (TRP) channels present in nociceptive neurones. As a consequence of the reduction of TTX-R VGSC currents, t-MrVIa transgenic mice display decreased inflammatory mechanical hypersensitivity, cold pain insensitivity and reduced firing of cutaneous C-fibres sensitive to noxious cold temperatures. These data validate the use of genetically encoded t-toxins as a powerful tool to manipulate VGSCs in specific cell types within the mammalian nervous system. This novel genetic methodology can be used for circuit mapping and has the key advantage that it enables the dissection of the contribution of specific ionic currents to neuronal function and to behaviour.

Abbreviations AP, action potential; BAC, bacterial artificial chromosome; DRG, dorsal root ganglion; GPI, glycophosphatidylinositol; IB4, isolectin-B4; PI-PLC, phosphatidylinositol-specific phospholipase C; t-MrVIa, membrane-tethered conotoxin MrVIa; TRP, transient receptor potential; TTX, tetrodotoxin; TTX-R, tetrodotoxin resistant; TTX-S, tetrodotoxin sensitive; VGSC, voltage-gated sodium channel; VGCC, voltage-gated calcium channel.

Introduction

Neuronal communication relies on action potentials (APs) generated by the activity of voltage-gated sodium channels (VGSCs) following membrane depolarisation. The alkaloid toxin tetrodotoxin (TTX) has been exploited for more than 40 years due to its unique ability to block VGSCs and therefore to assess the contribution of these channels to cell excitability and AP propagation. Nociceptive sensory neurones (nociceptors) detect noxious peripheral stimuli; this information is then transmitted to the superficial dorsal horn of the

spinal cord, relayed to the brain, and perceived as pain (Lewin & Moshourab, 2004). Nociceptors express two unusual VGSCs, $Na_v1.8$ and $Na_v1.9$, which are resistant to TTX (Dib-Hajj *et al.* 1998; Akopian *et al.* 1999). $Na_v1.8$ generates sodium currents with a high activation threshold (-40 mV) and slow inactivation (Sangameswaran *et al.* 1997; Akopian *et al.* 1999; Renganathan *et al.* 2002), whereas $Na_v1.9$ produces a persistent current with a more hyperpolarised voltage dependence and ultraslow recovery from inactivation (Baker, 2005; Cummins *et al.* 2007). In addition nociceptors are enriched in the $Na_v1.7$ TTX-S VGSC subtype (Nassar *et al.* 2004) which produces

the threshold currents (Matsutomi *et al.* 2006). Small molecules that specifically block the function of these VGSC subtypes include chemical tools (Jarvis *et al.* 2007), small interfering RNAs (Dong *et al.* 2007), and venom-derived toxins (Terlau & Olivera, 2004). The μO-conotoxins MrVIa and MrVIb were the first group of peptide toxins reported to inhibit VGSC currents in mammalian dorsal root ganglia (DRG) neurones (Daly *et al.* 2004). MrVIa was found to inhibit TTX-R VGSC currents with an IC_{50} value of $\sim$80 nM and a $\sim$10 times higher IC_{50} value ($\sim$1 μM) for TTX-S sodium currents (Daly *et al.* 2004; see Supplemental material associated with the current paper, Table 1, available online only).

In this study we have used the tethered toxin approach (Ibañez-Tallon *et al.* 2004; Holford *et al.* 2009) combined with cell-specific transgenesis, to deliver a genetically encoded tethered form of the neurotoxin MrVIa to nociceptors in mice. We show that this approach can be successfully used to manipulate VGSC currents in a cell-autonomous manner. Furthermore, the nociceptor-specific inhibition of VGSC currents in these transgenic mice leads to specific changes in the firing of noxious cold-sensitive nociceptors and reduction in inflammation-induced pain behaviour.

Methods

Mice were housed in the animal facility of the Max-Delbrück Center with *ad libitum* access to food and water in an air-conditioned room at 22–23°C with a standard 12 h light/dark cycle. Mice were killed by placement in a CO_2-filled chamber for a 2–4 min followed by cervical dislocation. All procedures conformed to the German guidelines of animal experimentation laid down by the government. Animal housing and care, as well as protocols for killing mice, are registered with and approved by the appropriate German federal authorities (Landesamt für Gesundheit und Soziales), which also governed proper implementation.

Generation of Tg-t-MrVIa bacterial artificial chromosome (BAC) transgenic mice

The mouse BAC clone (RP23-214H2) encompassing the *Scn10a* gene (Invitrogen) was modified to include the *t-MrVIa* expression cassette using the two-step recombination system (Gong *et al.* 2002). After electroporation and homologous recombination, resolved clones were screened by PCR and Southern blotting. The modified BAC for injection was purified by CsCl, linearised and 3 ng μl^{-1} of BAC DNA was injected into fertilised oocytes of hybrid BDF mice.

Southern blot analyses

Genomic DNA (5 μg) from each transgenic founder line was digested with *Nco*I and separated by gel electrophoresis. After gel denaturation (0.5 M NaOH, 1.5 M NaCl) and equilibration (10 $\times$ saline–sodium citrate buffer (SSC)), membrane blotting (Hybond N+ from Amersham) was performed in 10 $\times$ SSC. The membrane was quickly washed in 2 $\times$ SSC, dried for 2 h and crosslinked with UV light (Hoefer). DNA probes were radioactively labelled with α-^{32}P-dCTP (NEN) using the Prime-It RmT Random Primer Labeling kit (Stratagene). Twenty-five nanograms of the probe was purified via Probe-Quant G50 micro-columns (Amersham) and denatured at 95°C for 5 min before hybridisation. Hybridisation was performed at 65°C overnight in 5 $\times$ Denhardt's solution, 6 $\times$ SSC, 0.5% SDS and 100 μg ml^{-1} salmon sperm DNA. The membrane was washed in 2 $\times$ SSC/0.1% SDS followed by stringent washes in 0.1 $\times$ SSC/0.1% SDS. Autoradiograms were exposed at -70°C for 3 days.

Reverse Transcription PCR (RT-PCR)

Mouse tissues were rapidly dissected, collected in Trizol and homogenised. Total RNA was extracted by phenol/chloroform and treated with DNaseI (Invitrogen). RT-PCRs were performed using one-step platinum RT-PCR (Invitrogen). Primer pairs used were: t-MrVIa-F: 5′-TGGGAGTACTGCATAGTGCCGAT-3′, t-MrVIa-R: 5′-CCCGTAGTTCCATCCTTCCTTCAA-3′; Na_v1.8-F: 5′-TAACGTGTGGGTCTCTGTGC-3′, Na_v1.8-R: 5′-AGGTATGGAGCCAGGTCCTC-3′; β-actin-F: 5′-TCGTGCGTGACATCAAAGAGAAGC-3′, β-actin-R: 5′-ATGGATGCCACAGGATTCCATACC-3′.

In situ hybridisation

RNA probes were synthesised with T7 RNA polymerase using DIG labelling (Roche) and purified with the RNeasy kit (Qiagen). Dorsal root ganglia (DRG) from neonatal mice were collected in ice-cold PBS and frozen in OCT (Sakura). Cryosections were cut with 12 μm thickness. *In situ* hybridisation was performed with DIG-labelled probes as described (Muller *et al.* 2005).

Patch-clamp electrophysiology and data analysis

Whole-cell patch-clamp recordings were performed on DRG cultures from P7–P15 mice as previously described (Hu & Lewin, 2006) and 100 ng ml^{-1} nerve growth factor was added to the culture medium. Recordings were done 4–24 h after plating, using borosilicate capillaries with a resistance of 5–8 MΩ. For VGSC recordings, cells were

perfused with extracellular solution containing (in mM): 140 NaCl, 4 KCl, 1 $MgCl_2$, 2 $CaCl_2$, 4 glucose, 10 Hepes (pH 7.4) and pipettes were filled with solution containing (in mM): 122 KCl, 10 NaCl, 1 $MgCl_2$, 1 EGTA, 10 Hepes (pH 7.3). PI-PLC (Prozyme) was applied with 10 μg ml^{-1} for 1 h at 37°C. TTX experiments were performed with 0.5 μM TTX. Membrane potentials were kept at −60 mV, prepulsed to −120 mV for 150 ms and depolarised from −50 to +40 mV for 50 ms in increments of 10 mV. For current clamp analyses, neurones were held at resting membrane potential and current injection was increased from 80 pA in 80 pA increments. For VGCC recordings, the bath solution was replaced with (mM): 140 TEA-Cl, 2 $CaCl_2$, 10 Hepes, 10 glucose and 100 nM TTX, pH 7.4 with TEA-OH. The pipette solution contained (mM): 120 CsCl, 4 $MgCl_2$, 10 Hepes, 10 EGTA, pH 7.3 with CsOH. Currents were activated by 100 ms depolarisation pulses from a holding potential of −80 to 0 mV with 10 s intervals. Recordings were performed using an EPC10 amplifier (HEKA) at a sampling rate of 50 kHz. The series resistance was compensated for 40–60%. Data acquisition and analysis were performed with Patchmaster and Fitmaster software (HEKA Electronics, Darmstadt, Germany).

Skin–nerve assays

Single afferent units of the saphenous nerve from adult mice were identified using a mechanical stimulus (Milenkovic *et al.* 2008). C-fibres were subsequently examined for responsiveness to a cold ramp in which the temperature decreased from 30 to 0°C. Experiments were carried out blind, i.e. the genotypes of the mice were not known to the experimenter. Cold stimuli were delivered with a computer-controlled Peltier device in contact with the skin receptive field.

Electroporation and immunostaining of DRG cultures

DRG neurones were isolated from an adult mouse and cultured as previously described (Hu & Lewin, 2006). Two hundred micrograms per millilitre of biotinylated isolectin-B4 (IB4; Vector Labs) were used for IB4 live-stainings. DRGs were electroporated (Amaxa) with 5 μg of the pCS2+ eukaryotic expression plasmid containing t-MrVIA (CS2-t-MrVIA) and 0.5 μg of pCS2+ plasmid encoding the green fluorescent protein (CS2-EGFP) and plated on poly-L-lysine–laminin-coated coverslips. One day later, cells were fixed with 4% paraformaldehyde (PFA) and washed in PBS. Three per cent goat serum was used for blocking. The following antibodies and markers were used: mouse anti-FLAG (Sigma) at 1:1000, wheat germ agglutinin (Molecular Probes) at 1:200 (5 μg ml^{-1}), goat anti-mouse-Alexa 633 (Molecular Probes) at 1:400. Pictures were taken on a Zeiss LSM confocal microscope.

Transfection and immunoprecipitation in HEK293-T cells

HEK293-T cells were transfected with the CS2-t-MrVIa expression vector using lipofectamine 2000 (Invitrogen) according to the manufacturer's instructions. Immunoprecipitation with FLAG agarose beads (Sigma) and Western blot assays were performed as described (Ibañez-Tallon *et al.* 2002).

Immunostaining of spinal cord sections

Mice ($n = 1$ per genotype) were anaesthetized by intra-peritoneal injection of 500 μl of 5 mg Ketavet/200 μg Rompun in saline. Reflex responses such as limb withdrawal to paw pressure were used to indicate the need for a further dose of anaesthetic. Mice were then perfused with 4% PFA and cryosections were cut with 14 μm thickness. Mouse sections were blocked with 3% goat serum in PBS. The following antibodies and marker were used for immunostaining: rabbit anti-subP (Zymed Laboratories) at 1:1000, isolectin-B4–Alexa 488 (Vector Labs) at 1:500 and horse anti-rabbit–Alexa 594 (Molecular Probes) at 1:1000.

Calcium imaging

Standard fura-2-based ratiometric calcium imaging was used to record responses of DRG neurones cultivated from either wild-type or Tg-t-MrVIa mice (2–5 weeks of age) to application of different TRP channel agonists: capsaicin (TRPV1, 100 nM, 30 s), menthol (TRPM8, 100 mM, 30 s) and cinnamaldehyde (TRPA1, 100 mM, 30 s). KCl (40 mM, 10 s) was applied at the end of experiments and only cells exhibiting a robust response were analysed. An inverted microscope (Zeiss Observer A1) equipped with a MetaFluor photonics imaging system, including Poly-chromator V, and a CoolSNAP ES camera (Visitron) was used for cell imaging. Mouse genotype was unknown to the experimenter.

Frog surgery and oocyte recordings

Xenopus laevis female frogs ($n = 5$) were anaesthetized by immersion for 30 min in a 0.35% tricaine (Roth, Karlsruhe, Germany) solution until the animals were completely immobile and no further reflex limb withdrawal was detected. Frogs were rinsed in water before surgery and kept on ice during the surgery procedure. A relatively small piece of ovary was taken after performing a 1–2 cm-long abdominal incision through the overlying skin and a second incision through the muscles. The muscular incision was closed with DS16-5USP re-absorbable sterile surgical thread (Catgut GmbH). The skin incision was closed with DS16-5USP

non-absorbable sterile surgical thread (Catgut GmbH) and removed at the next surgery. After surgery frogs were kept for one day of observation in the laboratory before being returned to the main aquarium. The preparation of *Xenopus laevis* oocytes, cRNA transcripts and two-electrode voltage clamp recordings were conducted as described previously (Ibañez-Tallon *et al.* 2002). VGSC subunit cRNAs alone or with tethered toxins (ratio channel:toxin was 1:4) were injected into oocytes and recorded 3–5 days later.

Electron microscopy

Mice ($n = 2$ per genotype) were anaesthetized by intra-peritoneal injection of $500\,\mu$l of 5 mg Ketavet/200 μg Rompun in saline. Reflex responses such as limb withdrawal to paw pressure were used to indicate the need for a further dose of anaesthetic. Saphenous nerves were isolated from mice which had been perfused with 4% paraformaldehyde and postfixed in 4% paraformaldehyde/2.5% glutaraldehyde in PBS. Following treatment with 1% OsO$_4$ in 0.1 M phosphate buffer for 2 h for osmication, tissue samples were dehydrated in a graded ethanol series and propylene oxide and embedded in Poly/BedR 812 (Polysciences, Inc., Eppelheim, Germany). Semi-thin sections (1 μm) were stained with toluidine blue. Ultra-thin sections (70 nm) were contrasted with uranyl acetate and lead citrate. The numbers of non-myelinated and myelinated axons in the saphenous nerve of wild-type and transgenic mice were determined by the counting of 12 random fields under the electron microscope and normalising to total cross-sectional nerve area observed in semi-thin sections.

Behavioural experiments

Mice were backcrossed to C57/BL6/J for at least five generations. *Motor coordination*: motor coordination was assessed by placing the mice on an accelerating rotarod apparatus (Ugo Basile, Italy). Animals were scored for time to fall. *Thermal nociception*: thermal latency was determined using the Plantar test (Ugo Basile) (Hargreaves *et al.* 1988). Fifteen minutes after placing the mice in the Plexiglas chamber a high intensity light beam was directed at the plantar surface of the hindpaw. Movement of the paw stopped the light beam and the latency was indicated on a digital screen. Measurements were made five times on each paw and mean values were used for statistical analysis. *Mechanical nociception*: mechanical sensitivity was determined using a dynamic plantar aesthesiometer (Ugo Basile, Milan, Italy). All animals were acclimatised to the behavioural testing apparatus for 15 min. An increasing mechanical force (1 g s^{-1}) was applied to the

plantar surface of the mouse hindpaw. Each paw was measured five times and mean values of the applied forces were determined and used for statistical analysis. *Cold nociception*: mice were placed onto a Peltier-cooled plate maintained at $0 \pm 1^{\circ}$C. The number of lickings and jumpings were determined during 90 s. *Preferential heat test*: mice had free access to two plates kept at 10°C and 30°C. The time spent on each plate was measured. *Inflammatory pain*: mice ($n = 10$ per genotype) were anaesthetized by isoflurane inhalation. Thirty microlitres of 2% carrageenan in saline (Fluka) was injected into the plantar surface of the mouse right hindpaw to induce inflammatory hyperalgesia. On the following 3 days mice were tested for responses to heat and mechanical stimuli as described for the acute pain studies. Mice were killed by placing in a box filled with 100% CO$_2$ at the termination of the tests.

Statistical analysis

Results are presented as means ± S.E.M. Unpaired *t* tests or two-way ANOVAs were used when indicated. $P < 0.05$ was considered statistically significant.

Results

To generate a membrane-tethered isoform of MrVIa (t-MrVIa) we inserted a nucleotide sequence coding for the mature toxin between the sequences coding for a secretion signal and a glycophosphatidylinositol (GPI) anchor signal (Ibañez-Tallon *et al.* 2004) (Fig. 1*A*). Tethered toxin expression in nociceptors was achieved by (BAC) transgenic methodology (Gong *et al.* 2002) using genomic DNA that contains the *Scn10a* nociceptor-specific gene encoding for the Na$_v$1.8 VGSC α-subunit. Figure 1*B* shows the diagram of the BAC containing the *Scn10a* gene and the homology boxes for recombination with the modified shuttle vector containing the t-toxin cassette. Four transgenic founder lines were identified by Southern blotting (Fig. 1*C*). Comparison of the endogenous *Scn10a* allele to the transgene band indicated that transgenic lines 2 and 27 had the highest BAC transgene copy number. We encountered breeding problems with transgenic line 27 in that very few transgenic mice were born, which may have been a non-specific effect due to the size or the site of transgene insertion. We thus used line 2 (*Tg(Scn10a-t-MrVIa)2Iit* referred to hereafter as Tg-t-MrVIa mice) for all further experiments.

    Tg-t-MrVIa mice express *t-MrVIa* and *Scn10a* in DRGs, but not in other tissues along the nociceptive pathway whereas wild-type littermates showed comparable levels of *Scn10a* transcripts in DRGs, but lacked *t-MrVIa* expression (Fig. 2*A*). As expected from the developmental pattern of *Scn10a* (Benn *et al.* 2001), *in situ* hybridisation

indicated that *t-MrVIa* transcripts were present during embryonic development (Fig. 2*B*). In adult mice, *t-MrVIa* transcripts were detected in small-diameter nociceptors, but not in large-diameter sensory neurones (Fig. 2*C*).

An important feature of membrane t-toxins is their cell-autonomous action. To assess, whether this property was maintained *in vivo*, we prepared DRG primary cultures, which contain a mixture of sensory neurone types e.g. nociceptors and mechanoreceptors. Nociceptors were discriminated from mechanoreceptors by measuring AP configuration using the whole-cell patch clamp technique (Fig. 2*L*; AP half-peak width >3.1 ms for nociceptors and <0.8 ms for mechanoreceptors; see online Supplemental Table 2) and cell soma size (<25 μm soma diameter for nociceptors and >25 μm for mechano-receptors; Supplemental Table 2) as previously described (Stucky & Lewin, 1999; Lawson, 2002). Representative traces of VGSC currents, evoked by step depolarisation in voltage clamp mode, in nociceptors and mechano-receptors of both Tg-t-MrVIa mice and wild-type littermates are shown in Fig. 2*D* and *G*. Current–voltage relations indicated a significant reduction of VGSC currents in nociceptors of Tg-t-MrVIa mice compared to wild-type littermates (Fig. 2*E*). In contrast, VGSC currents in mechanoreceptors of Tg-t-MrVIa mice were indistinguishable from those measured in mechano-receptors of wild-type (Wt) littermates (Fig. 2*G* and *H*). Normalisation of peak VGSC currents to cell capacitance indicated a $41.1 \pm 9\%$ reduction of peak current densities in nociceptors of Tg-t-MrVIa mice compared to controls (Wt: 413.7 ± 37.2 pA pF^{-1}, Tg-t-MrVIa: 243.5 ± 37.2 pA pF^{-1}, $n = 32$, $P < 0.05$). However, no difference was observed in mechanoreceptors (Wt: 306.9 ± 57.4 pA pF^{-1}, Tg-t-MrVIa: 332.8 ± 26.8 pA pF^{-1}, $n = 9$) (Fig. 2*I*; Supplemental Table 2). To exclude the possibility that the t-MrVIa toxin could be affecting other ion channels present in nociceptors besides VGSCs, we tested the functionality of VGCC (Fig. 2*J* and *K*) and TRP channels (Fig. 1 in online Supplemental material). Patch-clamp recordings of VGCCs performed by step depolarisations indicated no differences between nociceptors of Tg-t-MrVIa mice compared to wild-type littermates (Fig. 2*J*). Current–voltage relationships did not differ between nociceptors of Tg-t-MrVIa and wild-type mice with currents measured with increasing voltage steps from -50 to $+40$ mV, and maximal peak currents obtained at a voltage depolarisation from -50 to -10 mV (Wt: -1.11 ± 0.9 nA, Tg-t-MrVIa: -1.13 ± 0.8 nA, $n = 10$ each) (Fig. 2*K*). The functionality and incidence of the TRP channels: TRPV1, TRPM8 and TRPA1 was measured by fura-2-based imaging of increases in [Ca^{2+}]$_i$ in DRG neurones through the sequential application of the specific activators capsaicin, menthol and cinnamaldehyde (Supplemental Fig. 1*A* and *C*). No significant differences in the

percentage of DRG neurones responding to each agonist were observed between Tg-t-MrVIa mice compared to wild-type littermates (capsaicin: Wt $35.8 \pm 8.1\%$, Tg-t-MrVIa 35.5 ± 5.1; menthol: Wt $15.3 \pm 5.6\%$,
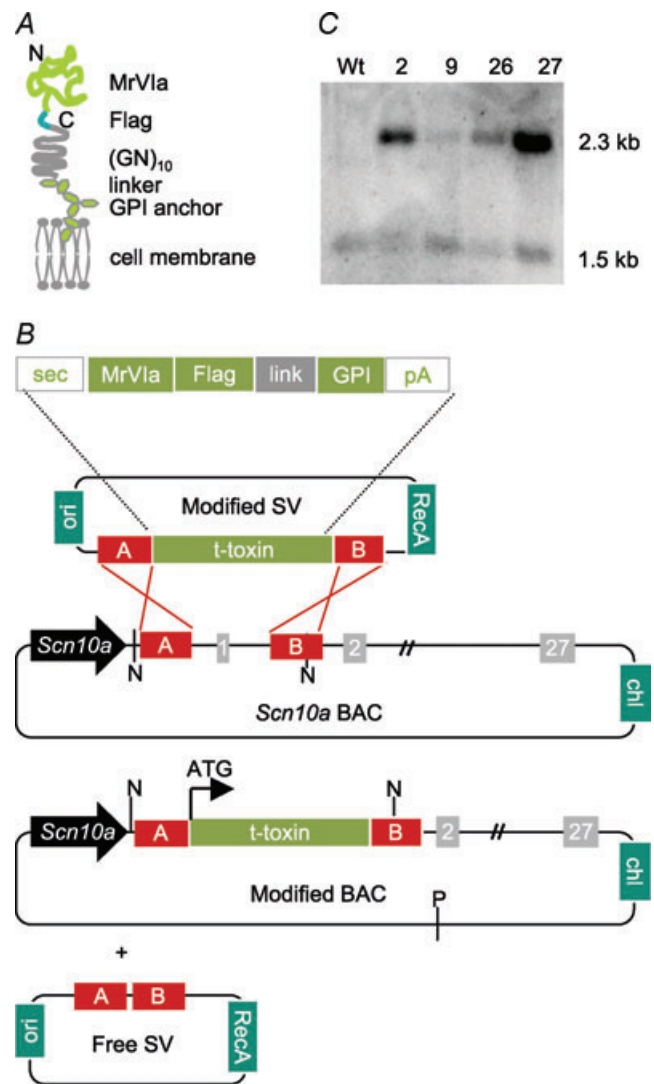

Figure 1. Generation of BAC transgenic mice encoding membrane-tethered MrVIa toxin

A, diagram showing t-MrVIa (green ribbon) including a FLAG epitope for immunodetection, a flexible poly (asparagine-glycine) linker (grey) and a GPI tether to the cell membrane. *B*, schematic overview of the BAC modification by two-step homologous recombination. The modified shuttle vector (SV) contains the t-toxin cassette (green), flanked by a secretion signal (sec) and a polyA (pA), inserted between two recombination boxes (A and B in red) corresponding to the sequences flanking the initiator methionine of the *Scn10a* gene encoding the Na$_v$1.8 VGSC subunit. Recombination (red lines) with the *Scn10a* BAC results in the modified BAC and the free shuttle vector. *Scn10a* gene promoter (black arrow), *Scn10a* exons (grey boxes), selection markers (dark green boxes), NcoI restriction sites for Southern blot (N), PI-SceI restriction site for BAC linearisation (P). *C*, Southern blot of transgenic founder lines. Lines 2 and 27 showed the highest relative ratio of the transgene band (~2.3 kb) in comparison with the endogenous *Scn10a* allele (~1.5 kb) indicative of high BAC copy number.
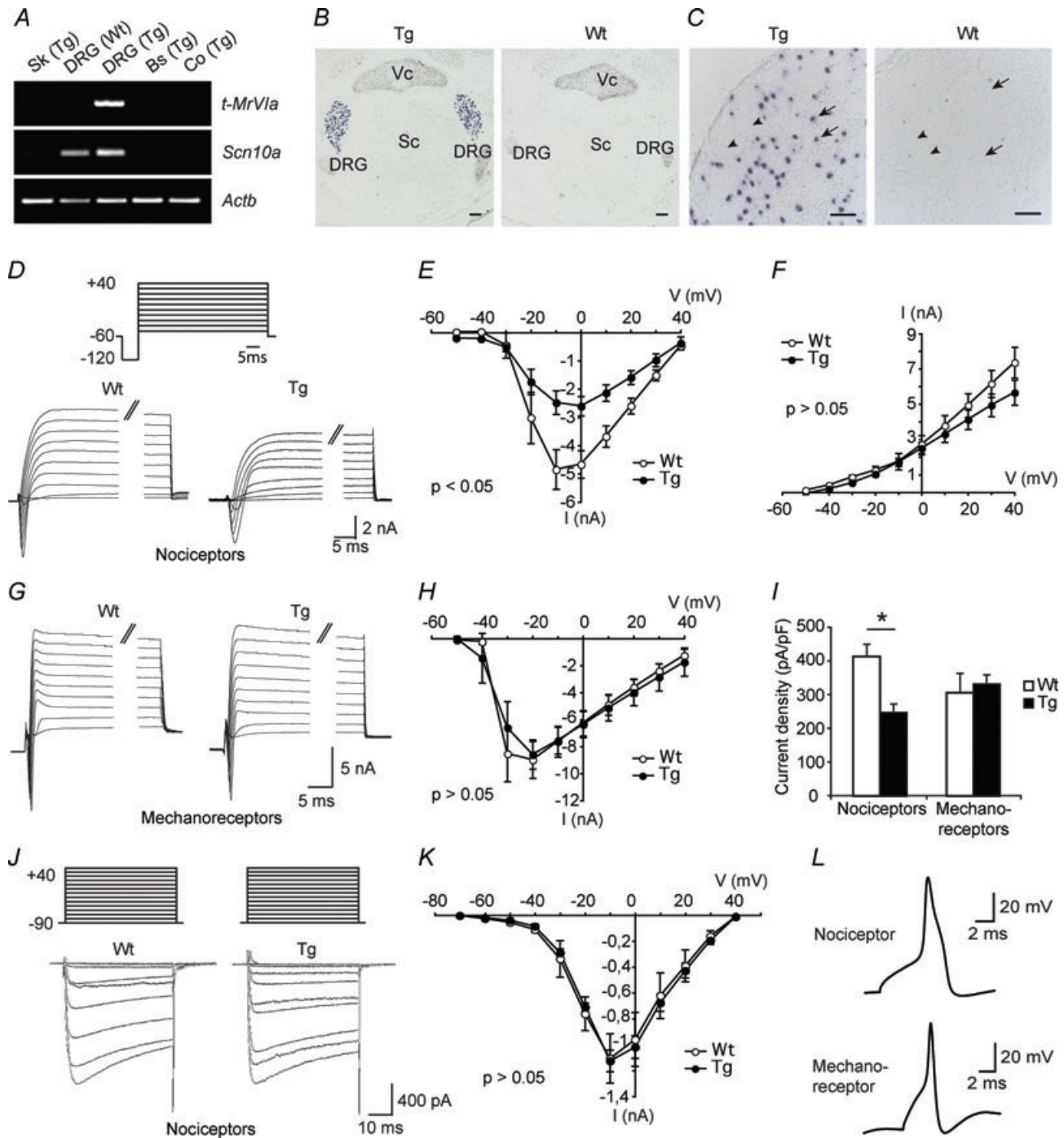
Figure 2. Cell-autonomous inhibition of sodium currents in nociceptors of Tg-t-MrVIa mice

A, co-expression of *Scn10a* and *t-MrVIa* transcripts in DRGs of Tg-t-MrVIa mice detected by RT-PCR analysis (Sk, skin; Bs, brain stem; Co, cortex. *B*, *in situ* hybridisation on spinal cord sections of mouse embryos (E15) show strong *t-MrVIa* signal in DRGs but not in spinal cord (Sc) of Tg-t-MrVIa mice. Vc, vertebral column. Scale bar: 100 μm. *C*, *t-MrVIa* transcripts were detected by *in situ* hybridisation in nociceptors (arrows) but not mechanoreceptors (arrowheads) of Tg-t-MrVIa mice (2–4 weeks old). Scale bar: 50 μm. *D–H*, voltage-gated currents were evoked by step depolarisations from −50 mV to +40 mV preceded by a hyperpolarizing prepulse from −60 to −120 mV to prevent inactivation. *D* and *E*, representative traces and current–voltage relationships of inward currents indicate a significant reduction of sodium currents in nociceptors of Tg-t-MrVIa mice in comparison to wild-type littermates. *F*, current–voltage relations of outward currents are not affected in nociceptors of Tg-t-MrVIa mice. *G* and *H*, representative traces and current–voltage relations of inward currents, evoked by the same protocol shown in *D*, indicate no differences in mechanoreceptors of Tg-t-MrVIa mice and wild-type littermates. *I*, peak

Tg-t-MrVIa 13.8 ± 4.0; cinnamaldehyde: Wt $10.1 \pm 6.6\%$, Tg-t-MrVIa 11.6 ± 6.2, $n = 4$ for both genotypes) (Supplemental Fig. 1*B* and *D*). These results show that these ion channels are not non-specifically affected by genetic expression of the t-toxin in these neurones. Other parameters, such as voltage-gated potassium outward currents (Fig. 2*F*) and the resting membrane potential (Wt -51.9 ± 1.95 mV, Tg-t-MrVIa -52.7 ± 1.1 mV, $n = 32$; Supplemental Table 2), were also unaltered in nociceptors of Tg-t-MrVIa mice compared to controls. These results indicate that t-MrVIa is cell autonomous and specific for VGSCs *in vivo*.

Nociceptors, electroporated with t-MrVIa and EGFP, showed FLAG immunolabelling at the cell membrane, which was abolished after treatment with phosphatidylinositol-specific phospholipase C (PI-PLC) that cleaves GPI-anchored proteins from the cell surface (Fig. 3*A*). Immunoprecipitation assays indicated that t-MrVIa is enriched in membrane fractions and cannot be detected in the culture medium (Fig. 3*B*). VGSC currents were measured before and after treatment with PI-PLC. Total peak current densities in nociceptors of Tg-t-MrVIa mice were restored to $87.5 \pm 8.6\%$ of control currents after PI-PLC (Fig. 3*C*). Taken together, these data demonstrate that t-MrVIa acts at the cell surface to block VGSCs.

A number of studies have reported that native MrVIa and its close relative MrVIb preferentially block TTX-R VGSCs, but at higher concentrations a subset of TTX-S channels are also affected by these toxins (Daly *et al*. 2004; online Supplemental Table 1). In Supplemental Table 1 we have presented an overview of the reported VGSC blocking capabilities of the native soluble forms of μO-conotoxins MrVIa and MrVIb in different experimental systems. These studies show that while the native conotoxins MrVIa/b are not highly selective for only one type of VGSC, they can discriminate between TTX-R channels present in nociceptors over TTX-S. Although the relative extent of the inhibition of VGSC current depends on the assay, and there is no direct comparison of all α-subunits within one experimental set of data, it would seem that native MrVIa/b preferentially blocks $Na_v1.8$ followed by $Na_v1.7$, $Na_v1.4$ and $Na_v1.2$. To determine whether the modified MrVIa used in this study maintains the characteristics of the native soluble MrVIa form, we performed oocyte electrophysiological assays with t-MrVIa and different VGSC α-subunits.

These experiments show significant block of $Na_v1.2$, but not of $Na_v1.1$, $Na_v1.3$ and $Na_v1.6$ VGSCs by t-MrVIa (Supplemental Fig. 2) in agreement with the reported affinities of the soluble toxin (Supplemental Table 1). Thus our experimental evidence suggests that the tether does not change the specificity of the MrVIa toxin.

We next used TTX to discriminate between TTX-R and TTX-S currents present in nociceptors. TTX-R currents in nociceptors of t-MrVIa transgenic mice show a $44 \pm 7\%$ reduction compared to wild-type mice (Wt: 284.3 ± 34.1 pA pF^{-1}, $n = 30$; Tg-t-MrVIa: 158.6 ± 20.4 pA pF^{-1}, $n = 31$, $P < 0.5$). This block was reversed by PI-PLC treatment thus demonstrating that the tethered toxin was responsible for this inhibition (PI-PLC: 243.6 ± 31.5 pA pF^{-1}, $n = 12$) (Fig. 3*C* and *D*). We observed a non-statistically significant inhibition ($31 \pm 13\%$; Wt: 129.6 ± 22.1 pA pF^{-1}, Tg-t-MrVIa: 89.3 ± 16.6 pA pF^{-1}, $P = 0.23$) of TTX-S currents in nociceptors with a very large sample size ($n = 32$ nociceptors recorded) (Fig. 3*C*). In addition the recovery of TTX-S currents after PI-PLC enzymatic cleavage of the tether was not statistically significant as it was for TTX-R currents. Thus the changes in TTX-S currents observed in transgenic mice might be indicative of partial (but not statistically significant) antagonistic activity of the t-MrVIa on these channels (Fig. 3*C*). Furthermore, we used a pulse protocol that avoids any substantial contamination by $Na_v1.9$, which undergoes ultraslow inactivation such that clamping the membrane potential for several minutes to at least -100 mV is required to release it from inactivation (Cummins *et al*. 1999; Amaya *et al*. 2006). Given that we used a holding potential of -60 mV while measuring TTX-R currents, similar to the experiments performed with the soluble toxin (Daly *et al*. 2004), our results demonstrate a block of $Na_v1.8$ TTX-R channels by t-MrVIa *in vivo*.

We next tested the effect of t-MrVIa on isolectin-B4 positive (IB4+ve) nociceptors, which have a higher density of TTX-R currents (Dib-Hajj *et al*. 1998; Stucky & Lewin, 1999; Snape *et al*. 2010). Voltage clamp analyses in DRG neurones live-labelled with fluorescently coupled IB4 indicated that the t-MrVIa-mediated block was $48 \pm 8\%$ in the IB4+ve neurone population (Wt: 422.7 ± 57.0 pA pF^{-1}, $n = 10$, Tg-t-MrVIa: 221.8 ± 33.2 pA pF^{-1}, $n = 12$) and $48 \pm 9\%$ in the IB4–ve population (Wt: 215.1 ± 33.6 pA pF^{-1}, $n = 20$;

VGSC current densities are significantly reduced in nociceptors of Tg-t-MrVIa mice (243.5 ± 37.2 pA pF^{-1}) with respect to wild-type mice (413.7 ± 37.2 pA pF^{-1}) ($n = 32$ per group) and unchanged in mechanoreceptors ($n = 9$ per group). $P < 0.05$ two-way ANOVA in *E* and *H*; $P > 0.05$ two-way ANOVA in *F*; $P < 0.05$ *t* test in *I*. *J* and *K*, representative traces (*J*) and current–voltage relations (*K*) of voltage-gated calcium currents, evoked by step depolarisations from -90 mV to $+40$ mV, indicate no differences in nociceptors of Tg-t-MrVIa mice and wild-type littermates ($n = 10$ per group). *L*, representative action potentials used to identify nociceptors and mechanoreceptors.
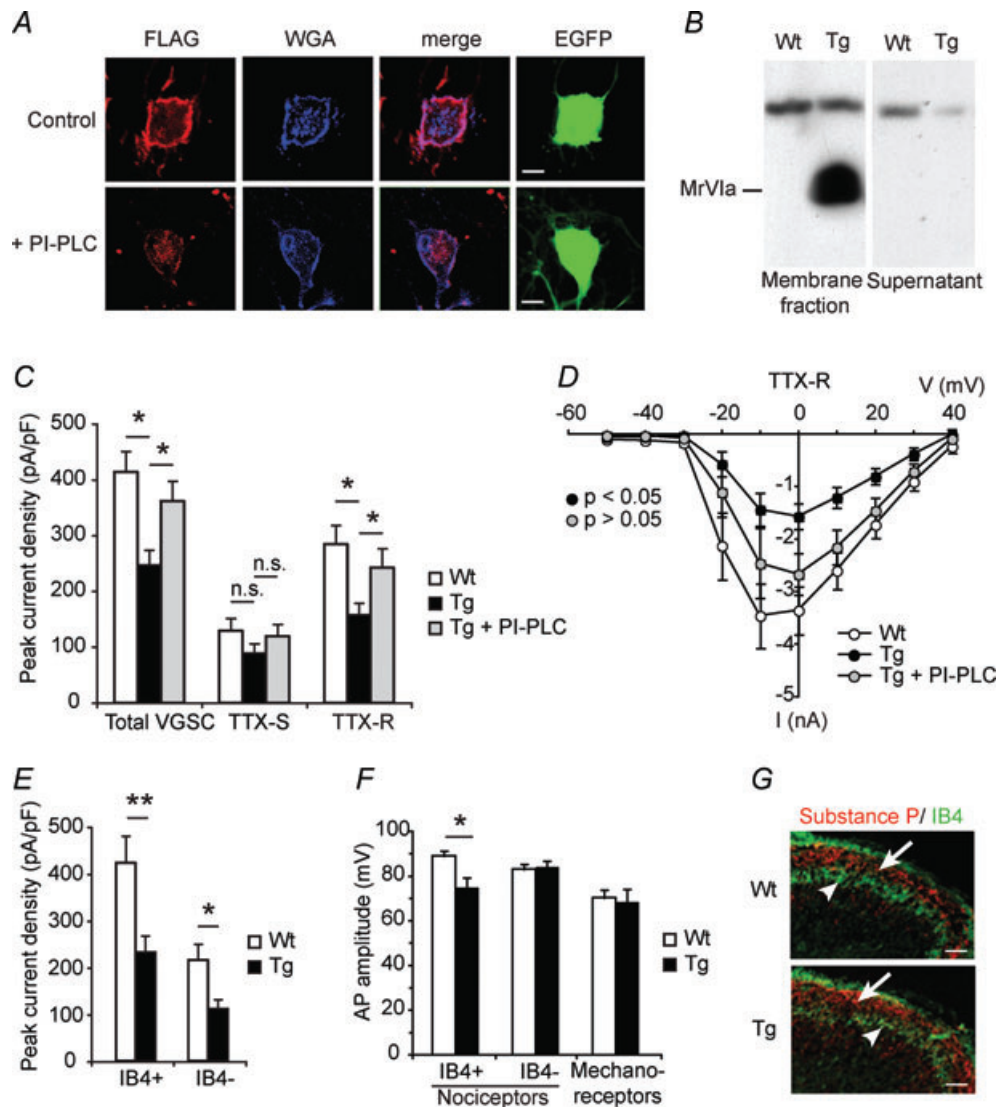
Figure 3. t-MrVIa acts at the cell membrane and specifically blocks TTX-R currents with no compensatory upregulation of other VGSCs

A, t-MrVIa (FLAG: red) colocalizes with the membrane marker WGA (blue) in DRG neurones co-electroporated with t-MrVIa and cytoplasmic EGFP (upper panel). PI-PLC treatment eliminates FLAG immunoreactivity showing specific cleavage of the GPI-anchored toxin from the membrane (lower panel). Scale bars: 5 μm. *B*, mammalian cells transfected with t-MrVIa show expression of the toxin in the membrane fraction by FLAG immunoprecipitation. *C*, bar graph indicating the quantification of VGSC peak currents in nociceptors of wild-type (Wt) and Tg-t-MrVIa mice ($n = 32$ cells per group) before and after TTX and PI-PLC treatment ($n = 12$ cells). The current densities of total VGSC and TTX-R currents are significantly reduced in Tg-t-MrVIa mice compared to wild-type mice, and significantly recover from t-toxin inhibition after PI-PLC treatment. TTX-S currents are not significantly affected in Tg-t-MrVIa mice. *D*, current–voltage relationships of TTX-R currents indicate a significant inhibition of sodium currents in nociceptors of Tg-t-MrVIa mice in comparison to Wt littermates ($P < 0.05$ two-way-ANOVA), and no significant inhibition, with respect to Wt, in Tg-t-MrVIa mice after PI-PLC treatment ($P > 0.05$ two-way ANOVA). *E*, peak current measurements in nociceptors treated with TTX and live-labelled with isolectin B4 indicate that IB4+ve nociceptors display more TTX-R than IB4–ve nociceptors in Wt and Tg mice and that t-MrVIa inhibition is significant in both subpopulations but more pronounced in IB4+ve nociceptors ($n = 10$–22 cells per group). *F*, the mean amplitude of action potentials is significantly reduced in IB4+ve nociceptors (Wt: 89.2 ± 2.3 mV, Tg-t-MrVIa: 74.3 ± 3.9 mV) but not in IB4–ve nociceptors and mechanoreceptors (*t* test). ($n = 9$–20 per group.) *G*, immunodetection of substance P (red) and isolectin B4 (green) in dorsal spinal cord indicate no differences in afferent innervation between Wt and Tg-t-MrVIa adult mice. Scale bar: 50 μm, *t* test in *C* and *E*.

Tg-t-MrVIa: $111.6 \pm 19.2\,\mathrm{pA\,pF^{-1}}$, $n = 19$) (Fig. 3E; Supplemental Table 2). TTX-R peak current densities were indeed higher in IB4+ve neurones (Fig. 3E) consistent with the reported higher content of $Na_v1.8$ in this cell population (Stucky & Lewin, 1999; Snape *et al.* 2010). We hypothesized that the t-toxin might have a stronger effect on IB4+ve nociceptors since the *Scn10a* gene promoter was used to genetically drive expression of the t-toxin. Therefore, we measured AP amplitudes in IB4+ve and IB4–ve nociceptors (Fig. 3F). Current clamp assays revealed that IB4+ve but not IB4–ve nociceptors from Tg-t-MrVIa mice had significantly reduced AP amplitudes ($\Delta = 14.9\,\mathrm{mV}$) (Fig. 3F; Supplemental Table 2). No significant changes in the number of myelinated or unmyelinated fibres (A-fibres: Wt 711.8 ± 3.1, Tg-t-MrVIa 714.8 ± 50.7; C-fibres: Wt 2920.6 ± 197.0, Tg-t-MrVIa 2660.7 ± 173.1; $n = 3$ mice; online Supplemental Fig. 3), and in the distribution of IB4+ve and IB4–ve nociceptor populations ($n = 2$ mice, online Supplemental Fig. 4) were observed. The central terminations in the outer laminae of the dorsal horn were also unchanged (Fig. 3G). In summary, t-MrVIa selectively reduces TTX-R VGSC currents in nociceptors in the absence of detectable morphological changes.

A battery of behavioural tests was performed on Tg-t-MrVIa mice. Motor activity and baseline sensitivities to noxious thermal and mechanical stimuli, as well as thermal hyperalgesia after inflammation, were normal (Supplemental Fig. 5; Fig. 4A). In contrast, mechanical hyperalgesia after inflammation, shown as the relative threshold for paw withdrawal before and after inflammation, was significantly reduced in Tg mice with respect to wild-type mice ($n = 10$ mice) (Fig. 4B), as was the nocifensive response to noxious cold (number of licks and jumps during 90 s on a $0°C$ plate: Wt 3.3 ± 0.9, Tg-t-MrVIa 1.2 ± 0.4) ($n = 10$ mice) (Fig. 4C; Supplemental Movies 1 and 2). No differences in behavioural thermoreception were observed (Fig. 4D). Thus, our data demonstrate that Tg-t-MrVIa mice have strong and specific deficits in nociception. We next asked whether the behavioural deficits we observed can be explained by changes in the stimulus–response properties of identified cutaneous nociceptors. We thus used the skin–nerve preparation to measure the firing frequencies of single cold-sensitive C-fibres. Two types of cold-activated fibres were recorded when subjected to a cooling gradient. A low-threshold population that started firing at innocuous temperatures ($\sim 25°C$, Fig. 4E) and a high-threshold population that started to respond only below $10°C$ (Fig. 4F). While the firing frequency in the low-threshold population did not differ between wild-type and Tg-t-MrVIa mice (Fig. 4E), the high-threshold population had significantly decreased firing rates during the cold ramp (Fig. 4F). Maximal differences were observed around $0°C$ in agreement with

our observations on noxious cold-evoked behavioural responses. The firing rates of C-fibres to noxious cold were significantly different in Tg-t-MrVIa mice, and were 4.5 ± 1.2 spikes $\mathrm{s^{-1}}$ ($n = 8$) in wild-type and 1.9 ± 0.5 spikes $\mathrm{s^{-1}}$ ($n = 4$) in Tg-t-MrVIa mice when the cold ramp reached $0°C$ (Fig. 4F). Thus our data indicate that TTX-R VGSC currents blocked by t-MrVIa in nociceptors are required both for nociception in the cold and for detection of noxious cold *per se*.

Discussion

This study establishes the utility of genetically encoded, cell membrane-anchored peptide toxins to dissect the contribution of VGSC conductances in a defined neuronal type *in vivo*, and thereby establish a causal link between cellular physiology and behaviour. We show that VGSC currents in nociceptors are cell-autonomously and selectively inactivated by t-MrVIa toxin and that this block can be reversed by enzymatic cleavage of the tether (Fig. 3). Within the targeted neuronal population, the t-toxin shows a high degree of specificity for TTX-R VGSCs and there was no evidence for compensatory changes in the activity of other ion channels present in the same neurones such as TTX-S VGSCs, VGCCs and TRP channels.

Detailed studies of $Na_v1.8$ and $Na_v1.7$ ion channel mutations have demonstrated the distinct roles of these channels *in vivo*, and compensatory mechanisms that are activated in abnormal physiological states (Akopian *et al.* 1999; Nassar *et al.* 2004; Rush *et al.* 2006). For example, analyses of $Na_v1.8$ knockout mice have shown that functional inactivation of $Na_v1.8$ is accompanied by a significant upregulation (about twofold) of TTX-S currents and a compensatory shift of the steady-state inactivation due to over-expression of *Scn9a* transcripts encoding the TTX-S VGSC $Na_v1.7$ (Akopian *et al.* 1999; Matsutomi *et al.* 2006). Here we asked whether a similar compensatory mechanism operates in Tg-t-MrVIa mice. As described above, partial inhibition of TTX-R currents in Tg-t-MrVIa was observed with no evidence of compensation by TTX-S currents. Interestingly the selective, but partial, block of TTX-R currents in the Tg-t-MrVIa mice described here resulted in pain-related phenotypes such as reduced mechanical hyperalgesia and insensitivity to noxious cold, which have been previously observed in $Na_v1.8$ null mutant mice and in *in vivo* models with selective inactivation of $Na_v1.8$ (Akopian *et al.* 1999; Jarvis *et al.* 2007; Zimmermann *et al.* 2007). However, while cutaneous fibres of $Na_v1.8$ null mutants show a significant reduction of menthol-sensitized cold responses (Zimmermann *et al.,* their Fig. 3G) and reduced firing rates when stimulated by constant mechanical pressure at low temperatures (Zimmermann *et al.*, their Fig. 3E and F) they do not show differences in cold-induced discharge

activity (Zimmermann *et al.*, their Fig. S6A). In our study we show that cutaneous fibres of Tg-t-MrVIa mice have significantly reduced firing rates after stimulation with cold ramps (from 25°C to 0°C) without the concurrent application of menthol, indicating that TTX-R VGSC currents sustain the ability of neurones to fire APs at very low temperatures. Thus the presence of TTX-R

VGSC current is not only responsible for the detection of mechanical stimuli in the cold, but also for the detection of noxious cold *per se*. The apparent discrepancy between our study and that of Zimmermann and colleagues might be attributed to the differences in the protocols used to measure cold-induced responses (a cooling ramp from 30°C to 10°C was used by Zimmermann *et al.*,
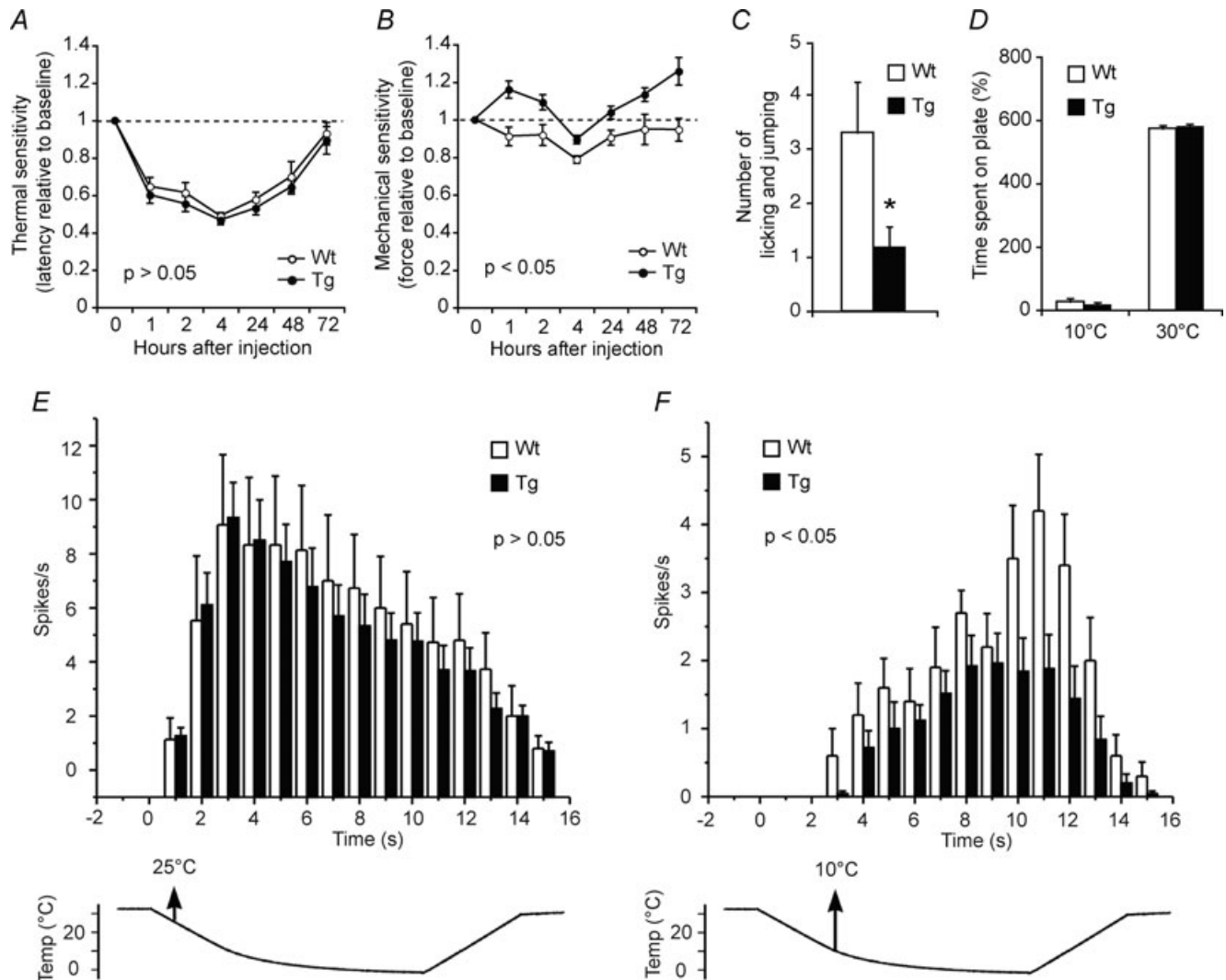
Figure 4. Tg-t-MrVIa adult mice show reduced inflammatory hyperalgesia and insensitivity to cold pain
A, no differences in inflammatory thermal hyperalgesia induced by intraplantar injection of carrageenan were observed between wild-type (Wt) and Tg-t-MrVIa mice (*n* = 10 mice). *B*, induced inflammation causes mechanical hyperalgesia in Wt mice (peak at 4 h) and significantly reduced hyperalgesia in Tg-t-MrVIa (*n* = 10 mice). Dashed line indicates baseline pain response. *C*, nocifensive cold responses scored during 90 s on a 0°C-cooled plate showed significantly reduced responses to noxious cold in Tg-t-MrVIa mice (*n* = 10 mice). *D*, temperature preference tests quantifying the time mice spent in either of two plates kept at 30°C and 10°C (*n* = 8 mice). *E*, histogram indicating the firing frequency of cold-sensitive C-fibres with a threshold >10°C over a cooling gradient from 30 to 0°C. The firing frequency did not differ between Wt and Tg-t-MrVIa mice (fibres: *n* = 8–12 fibres per group). *F*, histogram indicating the firing frequency of cold-sensitive C-fibres with a threshold < 10°C responding to noxious cold stimuli over a cooling gradient from 30 to 0°C. The firing frequency of cooling units with a threshold below 10°C is significantly reduced in Tg-t-MrVIa compared to Wt mice (fibres: *n* = 4–8 fibres per group). The lower trace corresponds to the cold ramp stimuli used in both cases. $P > 0.05$ two-way ANOVA in *A* and *E*; $P < 0.05$ two-way ANOVA in *B* and *F*; $P < 0.05$ *t* test in *C*.

while we used a ramp from 25°C to 0°C). Nonetheless when the cooling gradient reached 10°C we already observed reduced firing discharges in Tg-t-MrVIa mice (Fig. 4*E*). Since studies on $Na_v1.9^{-/-}$ null mutants have not indicated any contribution of these channels to cold sensitivity (Amaya *et al.* 2006), the t-MrVIa-mediated block of TTX-R currents resulting in cold insensitivity is presumably accounted for by blockade of $Na_v1.8$ exclusively. Studies on corneal C-fibres have shown that many cold-sensitive afferents sustain discharge to thermal stimulation even when TTX is applied to the preparation (Brock *et al.* 1998). It is thus quite possible that the residual TTX-insensitive current generated in the cutaneous endings of cold-sensitive fibres in the skin of transgenic mice is sufficient to preserve afferent responses to mild cooling. Environmental changes to innocuous cold temperatures are detected by the menthol TRPM8 receptor (Bautista *et al.* 2007). However, when temperatures become painful $Na_v1.8$ seems to be not only essential to maintain the excitability of nociceptors (Zimmermann *et al.* 2007), but based on our results the activity of $Na_v1.8$ is also required for nociceptors to detect noxious cold temperatures.

Nociceptor-specific VGSCs are important therapeutic targets and major efforts have been made to screen for specific molecules to block their function. For instance, conotoxins are already used as analgesic drugs. The MrVIa-related conotoxin MVIIa (commercialised as Prialt or ziconotide) is a specific antagonist of N-type VGCCs, and is used to treat patients with extreme neuropathic pain that is insensitive to opioids (Thompson *et al.* 2006). In contrast to local application of such analgesic peptides, delivered intrathecally via infusion pumps to avoid severe side effects due to diffusion of the toxin into the CNS, genetic delivery of tethered toxins to defined cell populations could become a viable alternate to prevent toxic effects and repetitive treatment. Future developments in the safety of gene transfer in humans offers considerable promise for the application of this novel tethered toxin technology to treat such extreme pain in humans. Extension of this approach to other peptide toxins together with the use of cell-specific genetic methods, may allow for specific intervention in defined neural circuits *in vivo* and therefore potential treatment of diseases caused by channelopathies.

Given the importance of VGSC function for AP propagation, the extensive use of TTX for functional inactivation of CNS neurones *in vivo,* and our demonstration that t-MrVIa can cell-autonomously inhibit VGSC function without resulting in misregulation of other ion channels or alterations in membrane potential, the extension of this methodology to other cell types and ion channels could provide a valuable new tool for the dissection of neural circuits. For instance, in a complementary study we have used other peptide toxins to block calcium influx through the VGCCs $Ca_v2.1$ and $Ca_v2.2$ (Auer *et al.* 2010). Thus, depending on the specificity and mode of action of the natural toxin of choice, this approach can be used for neuronal silencing by either inhibiting VGCCs and blocking neurotransmitter release (Auer *et al.* 2010), or, as in this study, inhibiting VGSCs and reducing cell excitability. Novel peptide toxin blockers specific for VGSC types present in the CNS ($Na_v1.6$ and $Na_v1.2$) have yet to be discovered, but once such tools become available our strategy could be then applied to effectively inactivate AP generation in central neurones. Thus, our study extends the range of available methodologies that can be used for genetic studies of neural circuitry (Luo *et al.* 2008). Furthermore, our technique represents a validated means to address the contribution of specific ion channels and receptors to neuronal function and behaviour.

References

Akopian AN, Souslova V, England S, Okuse K, Ogata N, Ure J, Smith A, Kerr BJ, McMahon SB, Boyce S, Hill R, Stanfa LC, Dickenson AH & Wood JN (1999). The tetrodotoxin-resistant sodium channel SNS has a specialized function in pain pathways. *Nat Neurosci* **2**, 541–548.

Amaya F, Wang H, Costigan M, Allchorne AJ, Hatcher JP, Egerton J, Stean T, Morisset V, Grose D, Gunthorpe MJ, Chessell IP, Tate S, Green PJ & Woolf CJ (2006). The voltage-gated sodium channel $Na_v1.9$ is an effector of peripheral inflammatory pain hypersensitivity. *J Neurosci* **26**, 12852–12860.

Auer S, Stürzebecher AS, Jüttner R, Santos-Torres J, Hanack C, Frahm S, Liehl B & Ibañez-Tallon I (2010). Silencing neurotransmission with membrane-tethered toxins. *Nat Methods* **7**, 229–236.

Baker MD (2005). Protein kinase C mediates up-regulation of tetrodotoxin-resistant, persistent Na^+ current in rat and mouse sensory neurones. *J Physiol* **567**, 851–867.

Bautista DM, Siemens J, Glazer JM, Tsuruda PR, Basbaum AI, Stucky CL, Jordt SE & Julius D (2007). The menthol receptor TRPM8 is the principal detector of environmental cold. *Nature* **448**, 204–208.

Benn SC, Costigan M, Tate S, Fitzgerald M & Woolf CJ (2001). Developmental expression of the TTX-resistant voltage-gated sodium channels $Na_v1.8$ (SNS) and $Na_v1.9$ (SNS2) in primary sensory neurons. *J Neurosci* **21**, 6077–6085.

Brock JA, McLachlan EM & Belmonte C (1998). Tetrodotoxin-resistant impulses in single nociceptor nerve terminals in guinea-pig cornea. *J Physiol* **512**, 211–217.

Cummins TR, Dib-Hajj SD, Black JA, Akopian AN, Wood JN & Waxman SG (1999). A novel persistent tetrodotoxin-resistant sodium current in SNS-null and wild-type small primary sensory neurons. *J Neurosci* **19**, RC43.

Cummins TR, Sheets PL & Waxman SG (2007). The roles of sodium channels in nociception: Implications for mechanisms of pain. *Pain* **131**, 243–257.

Daly NL, Ekberg JA, Thomas L, Adams DJ, Lewis RJ & Craik DJ (2004). Structures of μO-conotoxins from *Conus marmoreus*. Inhibitors of tetrodotoxin (TTX)-sensitive and TTX-resistant sodium channels in mammalian sensory neurons. *J Biol Chem* **279**, 25774–25782.

Dib-Hajj SD, Tyrrell L, Black JA & Waxman SG (1998). NaN, a novel voltage-gated Na channel, is expressed preferentially in peripheral sensory neurons and down-regulated after axotomy. *Proc Natl Acad Sci U S A* **95**, 8963–8968.

Dong XW, Goregoaker S, Engler H, Zhou X, Mark L, Crona J, Terry R, Hunter J & Priestley T (2007). Small interfering RNA-mediated selective knockdown of $Na_V1.8$ tetrodotoxin-resistant sodium channel reverses mechanical allodynia in neuropathic rats. *Neuroscience* **146**, 812–821.

Gong S, Yang XW, Li C & Heintz N (2002). Highly efficient modification of bacterial artificial chromosomes (BACs) using novel shuttle vectors containing the R6Kγ origin of replication. *Genome Res* **12**, 1992–1998.

Hargreaves K, Dubner R, Brown F, Flores C & Joris J (1988). A new and sensitive method for measuring thermal nociception in cutaneous hyperalgesia. *Pain* **32**, 77–88.

Holford M, Auer S, Laqua M & Ibañez-Tallon I (2009). Manipulating neuronal circuits with endogenous and recombinant cell-surface tethered modulators. *Front Mol Neurosci* **2**, 21.

Hu J & Lewin GR (2006). Mechanosensitive currents in the neurites of cultured mouse sensory neurones. *J Physiol* **577**, 815–828.

Ibañez-Tallon I, Miwa JM, Wang HL, Adams NC, Crabtree GW, Sine SM & Heintz N (2002). Novel modulation of neuronal nicotinic acetylcholine receptors by association with the endogenous prototoxin lynx1. *Neuron* **33**, 893–903.

Ibañez-Tallon I, Wen H, Miwa JM, Xing J, Tekinay AB, Ono F, Brehm P & Heintz N (2004). Tethering naturally occurring peptide toxins for cell-autonomous modulation of ion channels and receptors in vivo. *Neuron* **43**, 305–311.

Jarvis MF, Honore P, Shieh CC, Chapman M, Joshi S, Zhang XF, Kort M, Carroll W, Marron B, Atkinson R, Thomas J, Liu D, Krambis M, Liu Y, McGaraughty S, Chu K, Roeloffs R, Zhong C, Mikusa JP, Hernandez G, Gauvin D, Wade C, Zhu C, Pai M, Scanio M, Shi L, Drizin I, Gregg R, Matulenko M, Hakeem A, Gross M, Johnson M, Marsh K, Wagoner PK, Sullivan JP, Faltynek CR & Krafte DS (2007). A-803467, a potent and selective $Na_V1.8$ sodium channel blocker, attenuates neuropathic and inflammatory pain in the rat. *Proc Natl Acad Sci U S A* **104**, 8520–8525.

Lawson SN (2002). Phenotype and function of somatic primary afferent nociceptive neurones with C-, Aδ- or Aα/β-fibres. *Exp Physiol* **87**, 239–244.

Lewin GR & Moshourab R (2004). Mechanosensation and pain. *J Neurobiol* **61**, 30–44.

Luo L, Callaway EM & Svoboda K (2008). Genetic dissection of neural circuits. *Neuron* **57**, 634–660.

Matsutomi T, Nakamoto C, Zheng T, Kakimura J & Ogata N (2006). Multiple types of Na^+ currents mediate action potential electrogenesis in small neurons of mouse dorsal root ganglia. *Pflugers Arch* **453**, 83–96.

Milenkovic N, Wetzel C, Moshourab R & Lewin GR (2008). Speed and temperature dependences of mechanotransduction in afferent fibres recorded from the mouse saphenous nerve. *J Neurophysiol* **100**, 2771–2783.

Muller T, Anlag K, Wildner H, Britsch S, Treier M & Birchmeier C (2005). The bHLH factor Olig3 coordinates the specification of dorsal neurons in the spinal cord. *Genes Dev* **19**, 733–743.

Nassar MA, Stirling LC, Forlani G, Baker MD, Matthews EA, Dickenson AH & Wood JN (2004). Nociceptor-specific gene deletion reveals a major role for $Na_V1.7$ (PN1) in acute and inflammatory pain. *Proc Natl Acad Sci U S A* **101**, 12706–12711.

Renganathan M, Dib-Hajj S & Waxman SG (2002). $Na_V1.5$ underlies the 'third TTX-R sodium current' in rat small DRG neurons. *Brain Res Mol Brain Res* **106**, 70–82.

Rush AM, Dib-Hajj SD, Liu S, Cummins TR, Black JA & Waxman SG (2006). A single sodium channel mutation produces hyper- or hypoexcitability in different types of neurons. *Proc Natl Acad Sci U S A* **103**, 8245–8250.

Sangameswaran L, Fish LM, Koch BD, Rabert DK, Delgado SG, Ilnicka M, Jakeman LB, Novakovic S, Wong K, Sze P, Tzoumaka E, Stewart GR, Herman RC, Chan H, Eglen RM & Hunter JC (1997). A novel tetrodotoxin-sensitive, voltage-gated sodium channel expressed in rat and human dorsal root ganglia. *J Biol Chem* **272**, 14805–14809.

Snape A, Pittaway JF & Baker MD (2010). Excitability parameters and sensitivity to anemone toxin ATX-II in rat small diameter primary sensory neurones discriminated by *Griffonia simplicifolia* isolectin IB4. *J Physiol* **588**, 125–137.

Stucky CL & Lewin GR (1999). Isolectin B$_4$-positive and -negative nociceptors are functionally distinct. *J Neurosci* **19**, 6497–6505.

Terlau H & Olivera BM (2004). Conus venoms: a rich source of novel ion channel-targeted peptides. *Physiol Rev* **84**, 41–68.

Thompson JC, Dunbar E & Laye RR (2006). Treatment challenges and complications with ziconotide monotherapy in established pump patients. *Pain Phys* **9**, 147–152.

Zimmermann K, Leffler A, Babes A, Cendan CM, Carr RW, Kobayashi J, Nau C, Wood JN & Reeh PW (2007). Sensory neuron sodium channel $Na_V1.8$ is essential for pain at low temperatures. *Nature* **447**, 855–858.

Author contributions

Author's present address

J. Hu: Centrum für Integrative Neurowissenschaften (CIN), University of Tübingen, Paul-Ehrlich-Str. 15-17, 72076 Tübingen, Germany.